archives
of thermodynamics
Vol. **41**(2020), No. 1, 193–217
DOI: 10.24425/ather.2020.132955

Subcooled flow boiling of a citric acid aqueous mixture

MOHAMMAD AMIN ABDOLHOSSEIN ZADEH[a]
SHIMA NAKHJAVANI[b*]

[a] School of Engineering, University of South Australia, Australia
[b] School of Engineering, University of Yazd, Yazd, Iran

Abstract In the present research, an experimental investigation was conducted to assess the heat transfer coefficient of aqueous citric acid mixtures. The experimental facility provides conditions to assess the influence of various operating conditions such as the heat flux (0–190 kW/m^2), mass flux (353–1059 kg/m^{2}s) and the concentration of citric acid in water (10%–50% by volume) with a view to measure the subcooled flow boiling heat transfer coefficient of the mixture. The results showed that two main heat transfer mechanisms can be identified including the forced convective and nucleate boiling heat transfer. The onset point of nucleate boiling was also identified, which separates the forced convective heat transfer domain from the nucleate boiling region. The heat transfer coefficient was found to be higher in the nucleate boiling regime due to the presence of bubbles and their interaction. Also, the influence of heat flux on the heat transfer coefficient was more pronounced in the nucleate boiling heat transfer domain, which was also attributed to the increase in bubble size and rate of bubble formation. The obtained results were also compared with those theoretically obtained using the Chen type model and with some experimental data reported in the literature. Results were within a fair agreement of 22% against the Chen model and within 15% against the experimental data.

Keywords: Flow boiling; Heat transfer; Citric acid; Bubble formation; Chen type model

*Corresponding Author. Email: Shimaa.Nakhjavani@gmail.com

1 Introduction

Boiling heat transfer plays a major role in two-phase cooling systems and power cycles in which high-temperature and high-pressure steam production is generated. Boiling heat transfer mechanism includes several important subphenomena such as mixed convection-nucleate boiling heat transfer mechanisms, nucleation of bubbles, bubble formation, bubble growth and other phenomena. Considering the interaction of the bubbles, the boiling heat transfer becomes a complex heat transfer mechanism [1]. Boiling occurs when the vapor pressure of a liquid equals to the atmospheric pressure at its saturation temperature. Hence, a significant amount of heat needs to be transferred to the bulk of the liquid to push forward the liquid to enter the vapor phase through the bubble formation [2]. With the formation of the bubbles, the rate of heat transfer from the liquid to the vapor phase increases significantly, which is attributed to the phase change heat transfer and the amount of latent heat transferred between the liquid and vapour [3]. Therefore, the boiling heat transfer is considered as one of the potential mechanism for the high heat flux cooling systems [4–6]. However, there are challenges associated with the use of nucleate boiling heat transfer in two-phase systems:

1) The thermophysical properties such as heat capacity and thermal conductivity of the liquid materials are low, which results in a reduction of thermal performance of the system [7] or hinders the high rate of heat transfer within the bulk of the liquid [4,6,8,9].
2) In conventional single-phase cooling systems, the forced convective heat transfer is the dominant mechanism of heat transfer, which has a low heat transfer coefficient for the cases in which the heat flux is higher than 30 kW/m^2 [10–12].

Subcooled boiling is a phenomenon in which the temperature of the liquid is below its boiling temperature, however, a hot surface is immersed inside the liquid so that the local temperature of the liquid around the heating surface can be higher than the boiling temperature of the liquid. Hence, bubbles form around the heating section. However, the temperature of the bulk of the liquid is lower than the boiling temperature. Thus, the formed bubbles condense within the bulk of the liquid [13,14].

Recent studies have shown that subcooled flow boiling can be a suitable heat transfer mechanism for industrial applications due to its superior

heat transfer performance. In fact, removing the high amount of heat from a high heat flux medium via subcooled flow boiling is technically feasible since the heat transfer can occur in single or two-phase flow depending on the rate of heat flux applied to the system. However, there are some unknown phenomena in subcooled flow boiling heat transfer systems that have stimulated many researchers to conduct more research in this area. Boiling of liquid mixtures is one of the interesting options since it integrates the heat and mass transfer between the vapour inside the bubble and the vapour/liquid interface, which makes the phenomenon much more complicated. Much effort has been made to further develop an insight into subcooled boiling heat transfer of various liquids. For example, extensive studies have been conducted on pure liquids [15,16], binary and multi-components fluids [10,11,16–18] and nanofluids (various applications) [19–27] to develop an insight for better understanding the behavior of the system. Despite developing some promising models, they are unable to predict the heat transfer coefficient of subcooled boiling very well. This is because these models have been developed based on the limited number of data. Hence, there is a need for further investigations on subcooled boiling heat transfer to produce more data with a view to develop more generalized correlations [4–6,9,28–31]. Likewise, some assessments on the thermal performance of the boiling systems have revealed that the thermal performance of the system is limited to the type of the working fluid used in the system. This is because conventional fluids such as water or oil have a relatively poor thermal conductivity and low conductive/convective heat transfer coefficient. Thereby, researches were redirected to find new coolants with superior thermophysical properties (e.g., heat capacity and thermal conductivity) to be used in high heat flux applications. To review the state-of-the-art works on flow boiling of mixtures, following works in the literature are recommended [4,11,12,32,33]. According to the literature, binary mixtures can potentially have good thermal features and two-phase heat transfer behavior.

Amongst the binary mixtures assessed in the literature, citric acid aqueous mixture has been identified to have vast applications in boiler tube cleaning, hygienic industry and food science [34]. Hence, in the present work, the subcooled flow boiling heat transfer of aqueous citric acid mixtures was experimentally investigated. The influence of various operating conditions such as the heat flux applied to the boiling surface, the volumetric concentration of the citric acid in water (vol.%) and the mass flow rate

of the mixture on the heat transfer coefficient of the mixture was experimentally investigated. A visualization was also performed on the bubble formation with a view to analyze the influence of the heat and mass flux on the bubble formation in the mixture around the test section.

2 Experimental setup, data reduction and procedure

2.1 Test rig

Figure 1 presents a schematic diagram of the experimental setup used in the present research. The test rig consisted of a fluid loop, the main annular heat exchanger and the measurement instruments. A centrifugal pump (HP pumps Co., accuracy 1% of the reading flowrate) was utilized to circulate the citric acid-water mixture inside the cooling loop. An ultrasonic flow meter (accuracy 0.1% of reading) together with a bypass loop was utilized to measure and control the flow rate of the working fluid inside the system. The pressure and the temperature of the working fluid at the inlet and the outlet of the test rig was measured using two K-type thermocouples and two pressure transmitters (accuracy: 1% of the reading value), respectively. The outlet from the annular heat exchanger was cooled with a heat exchanger connected to a thermostat refrigerant bath with coolant temperature of 298 K.

The main test section was an annular heat exchanger consisting of a vertical stainless steel 316a rod installed inside a Pyrex tube equipped with eight thermocouples (Omega, accuracy of 0.1 K) located at various radial positions including 0, $\pi/4$, $\pi/2$, $3\pi/4$, π, $5\pi/4$, $3\pi/2$, and $7\pi/4$ to measure the surface temperature of the rod (see Fig. 2). The thermocouples have already been used and assessed in previous works and the accuracy of the reading values has already been validated in the previous publications [35–41]. To minimize the contact thermal resistance between the thermocouples and thermowells, a silicone paste with thermal conductivity of 5 W/(mK) was injected inside the thermowells. By doing this, the air is removed from the thermowells, while also the contact thermal resistance was minimized. Likewise, the pipes, valves and joints were heavily insulated with glass wool to minimize the heat loss from the system to environment. The arithmetic average of the temperature readings from the eight thermocouples was considered the initial surface temperature (T_{th}), which was used to estimate

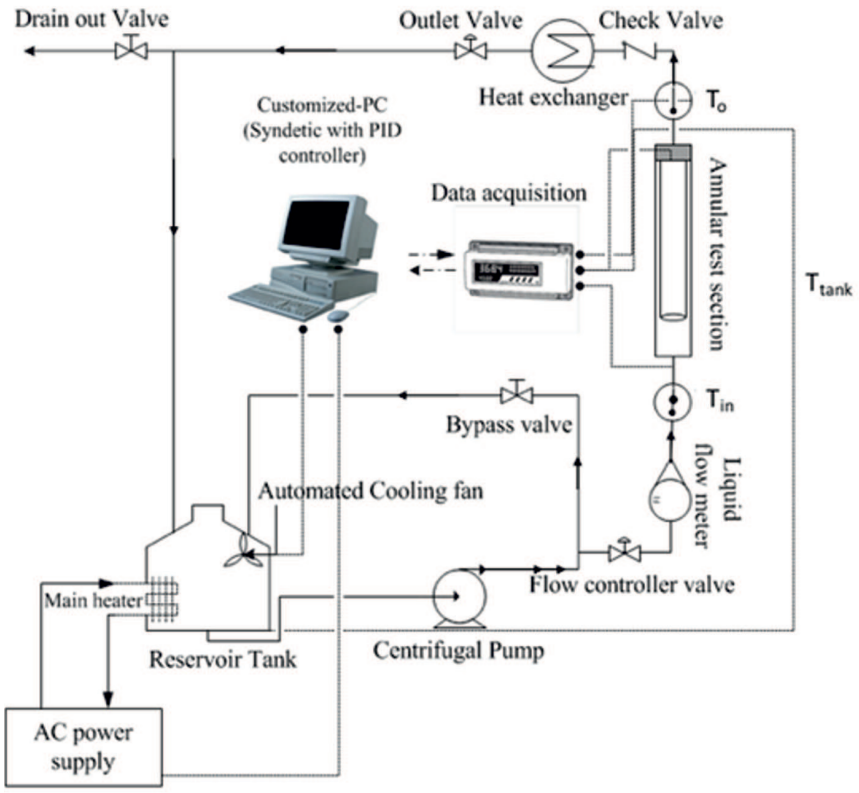

Figure 1: A scheme of test loop employed in this research [30].

the real surface temperature (T_w). Notably, the temperature was corrected because the thermocouples were not mounted exactly on the surface (see Fig. 2). Hence, the temperature readings from the thermocouples were amended using Eq. (2).

Also, the arithmetic average of the inlet and outlet temperature of the test section was considered as the bulk temperature of the citric acid mixture (T_b) [42]. The heat flux applied to the vertical stainless steel was provided with a cartridge heater placed inside the center of the stainless-steel rod. The gap between the heater and the rod was filled with silicone paste to minimize the thermal resistance. The voltage and current of the cartridge heater was maintained with an auto transformer (Emersun Co. 3000 Watt) equipped with an accurate multimeter to estimate the power of the cartridge heater.

All the thermocouples, the flow meter and the pressure sensors were connected to a data logger National Instrument (frequency of 1 kHz, 16 channels). The data logger was connected to a computer to process the data.

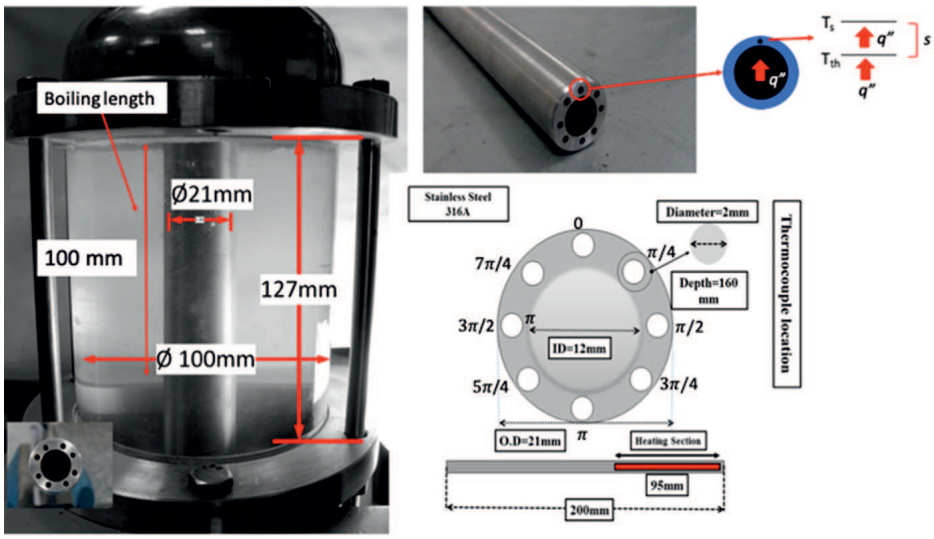

Figure 2: A schematic representation of the rod used in the present research [35].

Figure 2 represents the detailed specifications and geometrical properties of the annular heat exchanger. The diameter and length of the glass tube were 100 mm and 127 mm, respectively. The reason for using a glass tube was to enable one to take picture from the boiling phenomena and also the bubble formation. Likewise, the diameter and the total length of the stainless-steel pipe on which the boiling occurs were 21 mm and 130 mm, respectively. However, the boiling occurs on 100 mm of the vertical stainless-steel pipe (from the top side).

To capture the interaction of the bubbles and also to better understand the influence of the heat flux on the formation of the bubbles, a high-speed camera (EX-F1 Casio, 1200 frame per second) was employed and positioned in front of the vertical stainless steel rod to record the bubble interactions and the bubble formation. Also, a white ballast lighting system was utilized to provide sufficient light for taking images and to prevent any flickers and shadows within the images.

2.2 Data reduction and uncertainty

The subcooled flow boiling heat transfer coefficient, was calculated the following equation:

$$\alpha = \frac{\rho \dot{V} c_p \left(T_{out} - T_{in}\right)}{\left(T_w - T_b\right)} \, . \tag{1}$$

Here ρ is the density of the citric acid-water mixture, $\dot{V}$ is the volume of the citric acid-water inside the annular heat exchanger – $\dot{V} = A_h \vartheta$, where ϑ is the volumetric flow rate of the coolant in the annular space and A_h is the hydraulic cross section of the annular heat exchanger, which can be calculated as $\pi(D_o - D_i)^2/4$, in which D_o and D_i are 100 mm and 21 mm, respectively, where D_o and D_i are the outer and internal diameter of the annulus heat exchanger, respectively. However, in the present research $\dot{V}$ is directly measured with an ultrasonic flow meter. Also, c_p is the heat capacity, T is the temperature, the subscripts '*in*' and '*out*' stand for the inlet and the outlet of the test section, '*b*' and '*w*' stand for the film temperature and surface temperature, respectively. To calculate T_w, the following equation was used [11,18]:

$$T_w = T_{th} - q'' \frac{s}{k} \, , \tag{2}$$

where q'' is the heat flux applied to the rod, k is the thermal conductivity of stainless steel rod, s is the space between the thermocouple location and the surface of the rod, which is 2 mm (see Fig. 2). The heat flux was also calculated using the following equation [12,33]:

$$q'' = VI \, , \tag{3}$$

where, V is the voltage applied to the heater and I is the current of the heater circuit. The uncertainty of the experiments was estimated using Kline-McClintock equation [43] with the help of accuracies reported in the experimental section and Tabs. 1 and 2. As can be seen in Eq. (1), the uncertainty in the measurement of the heat transfer coefficient can be related to the errors in measurements of volume flow rate, hydraulic diameter, and the temperatures as follows:

$$\alpha = f\left\{\dot{V},\, A_h,\, \left(T_{out} - T_{in}\right),\, \left(T_w - T_b\right)\right\} \, , \tag{4}$$

$$\delta\alpha = \left(\left[\left(\frac{\partial \alpha}{\partial \dot{V}} \right) \delta \dot{V} \right]^2 + \left[\left(\frac{\partial \alpha}{\partial A_h} \right) \delta A_h \right]^2 \right. \tag{5}$$
$$\left. + \left[\left(\frac{\partial \alpha}{\partial (T_{out} - T_{in})} \right) \delta (T_{out} - T_{in}) \right]^2 + \left[\left(\frac{\partial \alpha}{\partial (T_w - T_b)} \right) \delta (T_w - T_b) \right]^2 \right)^{1/2},$$

where α is the subcooled flow boiling heat transfer coefficient, $\dot{V}$ is the volume flow rate, A_h is the cross section area of the annulus computed using the hydraulic diameter, ($D_h = 4A_h/P$, where P is the wetting area. T_{in}, T_{out} are fluid temperatures at the inlet and outlet of the annulus, respectively and T_w is the wall temperature of the heating section obtained from Eq. (2) and temperature readings from the thermocouples (T_{th}). Notably, for each parameter, δ represents its uncertainty. According to the above uncertainty analysis, the uncertainty in measurement of the heat transfer coefficient is 16.23%. The detailed information for the uncertainty analysis is gathered in Tabs. 1 and 2.

Table 1: Uncertainty of parameters used in the Kline-McClintock method.

Parameters	Uncertainty value	Unit
$\delta\dot{V}$	0.5×10^{-3}	m^3
δA_h	$2.5\times10^{-9*}$	m^2
$\delta(T_{out} - T_{in})$	0.3	K
$\delta(T_w - T_b)$	0.3	K

* In calculations, this value is zero.

According to the equation, the uncertainty of the heat transfer coefficient is 16.2%, uncertainty of the heat flux is 5.6%, uncertainty of heat loss to environment 4.2%. Any thermophysical properties of the mixtures were estimated using the correlations introduced in [44].

2.3 Experimental procedure

To conduct the experiments, the pipes, the fluid tank and the pump were washed with methanol and were flushed with deionized water to remove any dust and impurities from the test rig. Then, the citric acid mixture was prepared and loaded into the tank. The flow rate of the pump was set using bypass cycle and the flow meter. To apply the desired heat flux, the

Table 2: Summary of the uncertainty analysis related to instruments and devices.

Parameter	Uncertainty
Length, width and thickness, [m[	$\pm 5\times10^{-5}$
Temperature, [K]	0.1
Water flow rate, [lit. min^{-1}]	±1.5% of readings
Voltage, [V]	±1% of readings
Current, [A]	±0.02% of readings
Cylinder side area, [m^2]	$\pm 4\times10^{-8}$
Heat flux	5.6%
Mass flux	4.1%
Heat loss*	4.2%
Flow boiling heat transfer coefficient, [W/(m^2K)]	±16.2 %

*Obtained with the energy balance between the thermal input from the heater and the thermal energy exchanged inside the heat exchanger.

voltage was applied to the cartridge heater and the current of the heater was constantly monitored to avoid surcharge of the heater. A sufficient amount of time (10 min) was given to the system to reach a uniform and steady heat flux. Then, the temperature and flow rate were registered *via* a data logger. The experiments were conducted at various heat fluxes from 5 kW/m^2 to 190 kW/m^2, various volumetric concentration of citric acid in water (10% to 50%) and various mass flux to the annular heat exchanger (353 kg/(m^2s) to 1059 kg/(m^2s)). Notably, to be able to conduct a back-to-back comparison between the data, the temperature of the tank was set to 353 K during all the experiments. The imaging system was utilised to take images from the formation of the bubbles at various heat fluxes. Notably, to conduct a sensitivity analysis of a given operating parameter, the other operating parameters were kept constant, while the given operating parameter changed within the assumed range.

3 Results and discussion

3.1 Effect of heat flux

Figure 3 represents the variation of heat transfer coefficient with heat flux for various mass fluxes and for 10% volume fraction of citric acid in water.

As can be seen, with an increase in the heat flux, the flow boiling heat transfer coefficient nonlinearly increases. Two different regions can also be identified. The first region in which the heat transfer slightly increases with the heat flux referred to as 'the forced convective (FC) heat transfer domain'. The second domain is referred to as 'nucleate boiling (NB)', in which the heat transfer coefficient significantly increases with an increase in the heat flux. The enhancement in the heat transfer coefficient is largely due to the bubble formation and the local agitation due to the bubble interactions. For example, the heat transfer coefficient in the forced convective domain of heat flux 10 kW/m^2 is approx. 1600 W/(m^{2}K), while in the NB domain, for the same flow rate and of heat flux 100 kW/m^2 is approx. 5000 W/(m^{2}K).

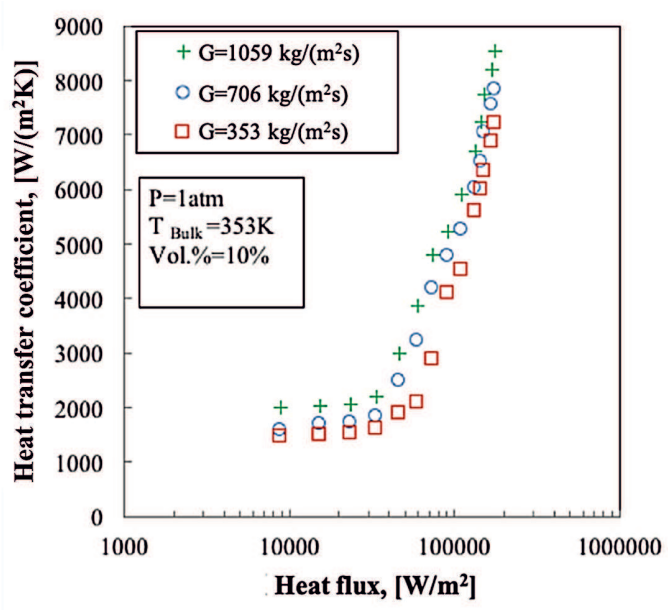

Figure 3: Influence of heat flux on flow boiling heat transfer coefficient for 10% citric acid in water.

As a definition, the onset of nucleate boiling is a point which separates the forced convective and the nucleate boiling heat transfer domains. At this point, the heat flux of the system is sufficient to increase the local temperature of the liquid above its boiling temperature. Hence, the first bubbles form on the surface, which might not be observable as they form and collapse within the liquid. This is because the bubble formation rate is

not high enough to create a column or a jet of the bubbles. However, both the bubble interactions within the liquid phase and the condensation heat transfer due to the conversion of the bubbles into liquid intensify the heat transfer coefficient. Therefore, the heat transfer coefficient after the ONB point (the nucleate boiling regime) is relatively higher than that measured before the ONB point (the forced convective heat transfer regime).

For better understanding, Fig. 4 represents the dependence of the heat transfer coefficient on the applied heat flux for 30% volume fraction and for various mass fluxes of citric acid-water mixture. As can be seen, the two heat transfer regions follow different trends as the slope of change for the FC domain is significantly lower than that observed for the NB region. Again, with an increase in the heat flux, the heat transfer coefficient increases and this trend is seen for all other volumetric concentrations of citric acid in water. Likewise, the ONB (onset of nucleate boiling) point is clearly identifiable from the figure. Notably, for all the experiments, the temperature of the tank is kept constant at 353 K. This provides a back-to-back comparison between the results obtained from the sensitivity analysis of the operating parameters.

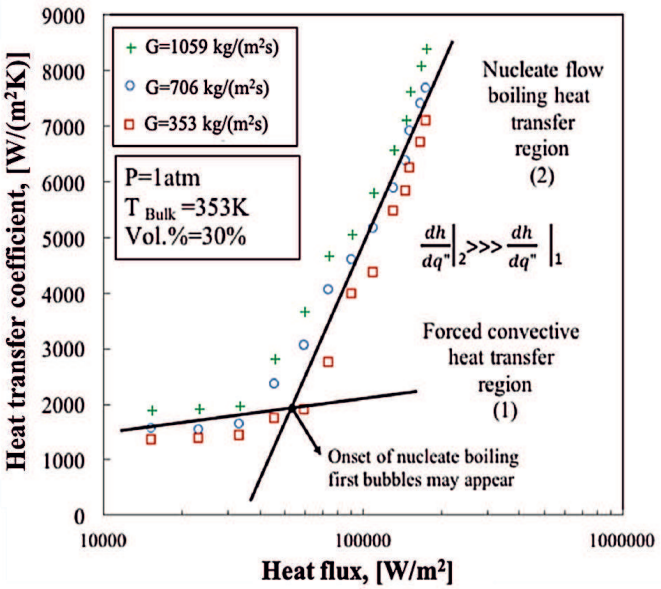

Figure 4: Dominant mechanisms of heat transfer in flow boiling of aqueous citric acid.

3.2 Effect of mass flow rate (mass flux)

It can be observed in Figs. 3 and 4 that with an increase in the flow rate (here, mass flux of the citric acid-water mixture), the heat transfer coefficient of the mixture increased. This behavior was seen for other heat fluxes, other volumetric concentrations of citric acid in water and also for other mass fluxes. It was also found that the increase in the mass flux of the mixture had no influence on the point of onset of nucleate boiling, while considerably changed the heat transfer coefficient. Notably, the rate of change in the NB region was relatively higher than that observed in the FC region. This was attributed to the presence of the bubbles inside the citric acid mixture, which created sufficient turbulence and also plausible interactions between the hot surface and the bulk of the mixture, thereby showing significant change in heat transfer coefficient in the nucleate boiling region.

3.3 Effect of volumetric concentration

Figure 5 represents the dependence of heat transfer coefficient on the heat flux for various volume fraction of citric acid in water in the forced convective region. As can be seen, with an increase in the volumetric concentration of the citric acid, the heat transfer coefficient decreases. For example, at heat flux of 50 kW/m^2, the heat transfer coefficient at a 10% volume fraction is approx. 2050 W/(m^{2}K), while it is approx. 1700 W/(m^{2}K) at 50%. This can be attributed to the mixture effect. In fact, for pure liquids, boiling is a heat transfer controlled phenomenon, while for mixtures, particularly binaries, the vapour phase is strictly enriched of the light component. Since the rate of mass diffusion is much slower than heat diffusion, the mass transfer of the light component(s) towards the bubble interface becomes the limiting factor and a portion of the driving force is consumed to overcome the mass transfer resistance [45–47]. Therefore, an additional temperature driving force is required for mixtures in comparison with pure liquids to reach the same thermal performance. Hence, a lower heat transfer coefficient is reported for the mixtures in the boiling processes. To validate the results, a rough comparison was conducted between the experimental data and those theoretically obtained with the help of a Dittus-Boelter equation, which is illustrated in Fig. 5a. Figure 5b presents the dependence of the temperature difference between the wall and the bulk temperature of the working fluid on the heat flux. As can be seen, with an increase in the heat flux applied to the surface, the temperature difference between the wall

and the bulk temperature of the liquid increases. The bulk temperature is set to 353 K for all the experiments. Hence, the minimum and maximum wall temperature of the surface are 276.05 K and 282.85 K for volumetric fractions of 50% and 10%, respectively. This is because the heat transfer coefficient is higher at a 10% volume fraction, which results in better heat transfer between the surface and the liquid. Hence, the temperature difference was smaller for a volumetric fraction of 10%. The similar behavior was also seen for other heat fluxes in the nucleate boiling region.

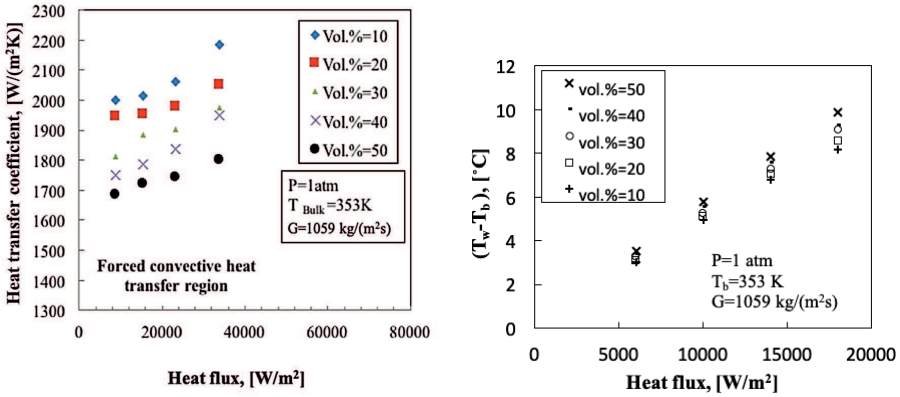

a) b)

Figure 5: Influence of the volumetric concentration of the citric acid in water on the heat transfer coefficient in the forced convective heat transfer region: a) heat transfer coefficient versus heat flux, b) temperature difference versus heat flux.

Figure 6 illustrates the comparison between the results obtained from the Dittus-Boelter equation and those experimentally obtained in the forced convective heat transfer region. As can be seen, a good agreement within a 12.83% margin is reported between the experimental data and those calculated from the correlations for the forced convective heat transfer domain. Also, a linear trend for the change in heat transfer coefficient with the heat flux was observed, which is in line with the results predicted from the equation.

Figure 7a presents the variation of heat transfer coefficient with the applied heat flux for the nucleate boiling heat transfer region. As can be seen, with an increase in the heat flux, the heat transfer coefficient increased. However, with the increasing volumetric fraction of citric acid the heat transfer coefficient decreases due to the mixture effect. To validate

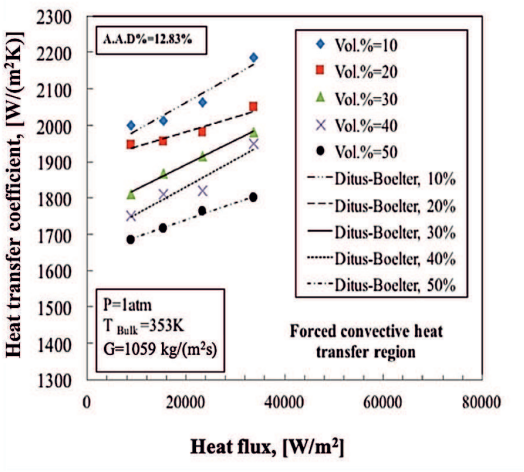

Figure 6: Comparison between the heat transfer coefficients obtained from the Dittus-Boelter correlation and from the experiment in the forced convective region.

the results, a rough comparison was made between the experimental data and those theoretically obtained with the Chen type model, discussed in the following section. Figure 7b illustrates the temperature difference between the wall and the bulk of the mixture for various heat fluxes in the nucleate boiling heat transfer regime. As can be seen, for the heat flux ranged from 35 kW/m^2 to 85 kW/m^2, the temperature difference is within the range of 284.7 K to 291.15 K. It means that the temperature of the wall is well above approx. 363 K, which is higher than the boiling temperature of the mixture (355–358 K for volumetric fractions between 10% and 50%). Hence, the boiling occurs around the surface. Also, it can be seen that the difference between the wall and the bulk temperature of the liquid is relatively larger than that observed for the forced convective region showing the plausible heat transfer occurring in the nucleate boiling heat transfer region. This, as discussed before, is attributed to the formation of the bubbles around the surface, which enhances the heat transfer rate from the surface to the bulk of the liquid.

3.4 Comparison with the Chen model

The Chen correlation is a relatively well-known model to estimate the nucleate boiling heat transfer coefficient for various types of liquids including

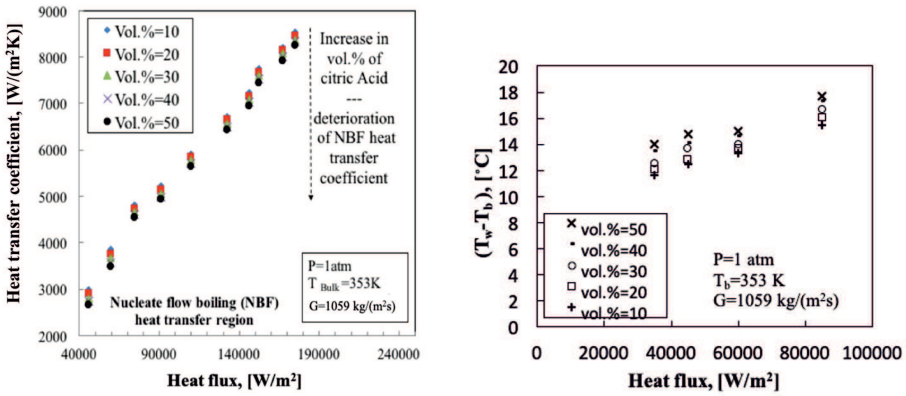

a) b)

Figure 7: Influence of volumetric concentration of citric acid in water on the heat transfer coefficient in nucleate boiling heat transfer region: a) heat transfer coefficient versus heat flux, b) temperature difference versus heat flux.

pure and binary mixtures [28]:

$$\alpha_{fb} = S\alpha_{nb} + F\alpha_{fc}\,. \tag{6}$$

Here α_{fc} is the forced convective heat transfer coefficient for the single-phase domain. F is a coefficient that accounts for the apparent increase in the velocity due to the presence of the vapour and is a function of the Martinelli parameter. α_{nb} is the pool boiling heat transfer coefficient at the local wall superheat and can be calculated using any pure liquid pool boiling predicting correlations. The suppression factor S accounts for the suppression of the nucleate boiling. The coefficient α_{nb} can be calculated with the pool boiling correlations. Notably, the pool boiling correlations over-predict the heat transfer coefficient, hence S is used to neutralize the over-prediction [42].

To calculate S and F, Coiller fitted the following equations to the graphical relationships for F and S [48]:

$$F = \begin{cases} 1 & \text{if } \frac{1}{X_{tt}} \leq 0.1\,, \\ 2.35\left(\frac{1}{X_{tt}} + 0.213\right)^{0.736} & \text{if } \frac{1}{X_{tt}} \geq 0.1 \end{cases} \tag{7}$$

and

$$S = \frac{1}{1 + 2.53 \times 10^{-6} N_{Re_{tp}}^{1.17}}\,. \tag{8}$$

The Martinelli parameter, X_{tt}, can be calculated from the following equation:

$$X_{tt} = \left(\frac{1-\dot{x}}{\dot{x}}\right)^{0.9} \left(\frac{\rho_{bf}}{\rho_{nf}}\right)^{0.5} \left(\frac{\mu_{nf}}{\mu_{bf}}\right)^{0.1} , \tag{9}$$

where ρ and μ are the density and viscosity, the substripts bf, nf denote base fluid and nanofluid. Here

$$N_{Re_{tp}} = \frac{\dot{m}\,(1-\dot{x})\,d_h}{\mu_{nf}}\,F^{1.25} , \tag{10}$$

where $\dot{m}$ is the mass flow rate of the coolant, $\dot{m}$ is the local vapour mass fraction and d_n is the hydraulic diameter. Further information on these equations can be found in [16,38,49]. The local vapour mass fraction is given as

$$\dot{x} = N_{ph} - N_{ph,n}\,\exp\left(\frac{N_{ph}}{N_{ph,n}} - 1\right) . \tag{11}$$

Here N_{ph} is the phase change number and is defined as

$$N_{ph} = \frac{h_v - h_{l\,,sat}}{h_{fg}} , \tag{12}$$

where N_{ph} is a value of the phase change number at a temperature at which the fluid can be in a two-phase condition, h_v, h_{fg}, and $h_{l,sat}$ are the enthalpy of vapour phase, enthalpy of evaporation and enthalpy of liquid in saturation temperature, respectively. For the present work, the phase change number was calculated at 353 K at which bubbles are clear to be captured with a high-speed camera. Schroder suggested calculating $N_{ph,n}$ from the following correlation using the boiling, Bo, and Peclet numbers [38,49]:

$$N_{ph\,n} = \frac{-N_{\mathrm{Bo}}}{\sqrt{\left(\frac{455}{N_{\mathrm{Pe}\,l}}\right)^2 + 0.0065^{\,2}}} , \tag{13}$$

where

$$N_{\mathrm{Bo}} = \frac{\dot{q}}{\dot{m}\;h_{fg}} \quad N_{\mathrm{Pe}} = \frac{\dot{m}\,C_{p,nf}\,d_h}{\lambda} , \tag{14}$$

where $\dot{q}$ is the heat flux, h_{fg} is the enthalpy of evaporation, $C_{p,nf}$ is the heat capacity of nanofluid.

The length from the beginning of the test section to the point at which the phase change number is zero is calculated as

$$\Delta L = \frac{-N_{ph\,o}\; d_h}{4N_{\mathrm{Bo}}}\;, \tag{15}$$

$$N_{ph_o} = \frac{-C_{p,nf}\,(T_{sat}\,-\,T_b)}{h_{fg}}\;, \tag{16}$$

where T_{sat} and T_b are the temperatures of saturation liquid and bulk liquid, respectively.

Using Eq. (16), the phase change number is calculated for the length at which boiling heat transfer occurs. Then, the characteristic length (ΔL) is calculated from Eq. (15). Having the value of ΔL, the length coordinate for the actual thermometer position (ΔL_t) can be calculated with the following equation:

$$\Delta L_t = \Delta L + x_{th}\;, \tag{17}$$

where x_{th} is the distance of thermocouple to the surface (position of the thermocouple). Notably, the boiling phenomenon occurs 0.11 m from the vertical stainless steel wall. However, the length of the thermocouples was 11 cm, hence $x_{th} = 0.01$ m. Thus, the phase change number at the thermometer location is:

$$N_{ph} = \frac{-4\,N_{Bo} \times \Delta L_t}{d_h}\;. \tag{18}$$

In order to calculate the flow boiling heat transfer coefficient (HTC), two equations are required for the forced convective and nucleate boiling domains. In the present work, we chose the Gnielinski equation [50] for the forced convection and Gorenflo correlation [51,52] for the nucleate pool boiling domain. The result of comparison with the Chen model is presented in Fig. 8. As can be seen, the experimental data are within 22% of the theoretical ones showing that not only our results are reliable, but that the Chen type model is a suitable model to predict the heat transfer coefficient of a mixture.

Figure 8 presents the results of comparison between the experimental data obtained in the present work and those reported in the literature for a similar test rig (annular heat exchanger) conducted by Sarafraz *et al.* [53,54] and those reported for the binary mixtures of water/ethylene amine (MEA) and water/ethylene glycol [55,56]. As can be seen, regardless of the type of working fluid, for the same heat flux and the same operating

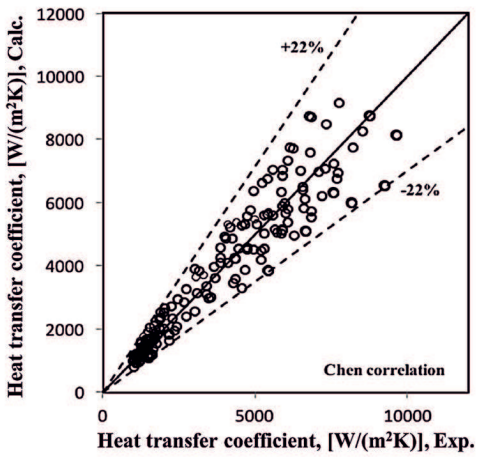

Figure 8: Comparison between Chen correlation's results and experimental data for flow boiling heat transfer coefficient.

conditions (e.g., temperature of 353 K), the measured was within the deviation of ±15% against the data available in the literature. This shows the trustworthiness and reliability of the reported data.

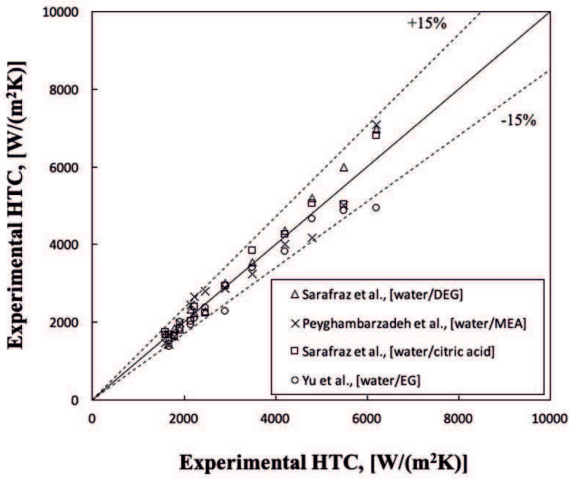

Figure 9: Comparison between the experimental data and those obtained from the literature.

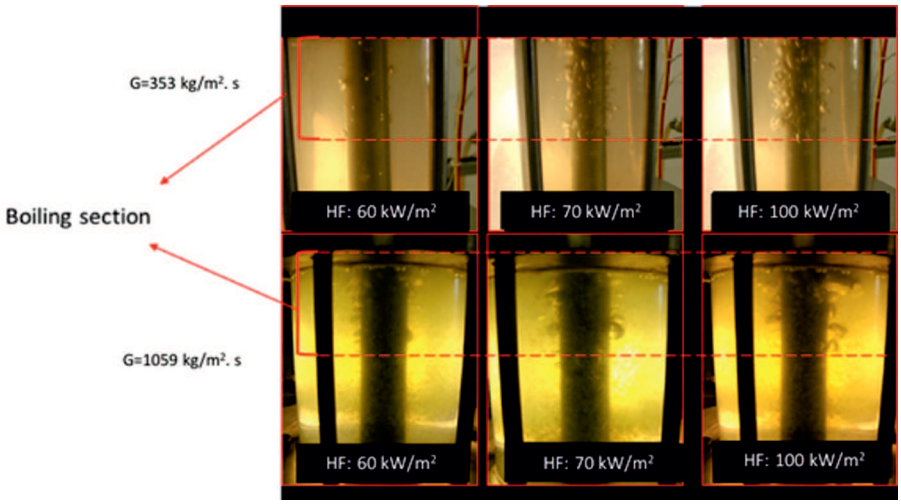

(a)

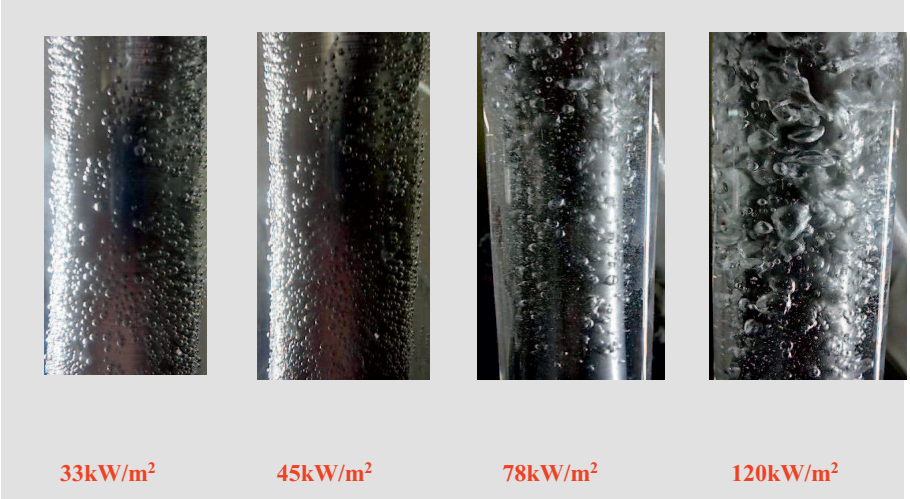

(b)

Figure 10: Bubble formation at different mass and heat fluxes for a 20% vol. of citric acid in water: a) various mass fluxes, b) various heat fluxes.

3.5 Bubble formation

Figure 10 illustrates the images of bubble formation in the nucleate boiling regime taken from the test section with a high speed camera at 1.200 frames per second. This camera has previously been used for the boiling tests and showed a great potential for assessing the high-speed phenomena in medical applications [57–61] and transport phenomena, including the bubble formation [23,24,62–65]. As can be seen, with an increase in the heat flux, the bubble formation was intensified. The bubbles were smaller at lower heat fluxes, while they became large at high heat fluxes. This was because at higher heat fluxes, the rate of evaporation of the base fluid increased, hence, more vapour was captured in the bubble resulting in increase in the mean size of the bubbles. Interestingly, the same behavior was observed at other flow rates. However, the flow rate slightly changed the rate of bubble formation. This is because at larger flow rates, the boiling microlayer adjacent to the heating surface was renewed quickly and as a result, the residence time for the bubbles to form and grow on the surface decreased. Also, it was found that at larger flow rates, the means size of the bubbles was smaller. Notably, the same behavior was seen for other volume fractions of citric acid in water.

As mentioned, the bubbles are larger at higher heat fluxes. This can be attributed to the superior heat transfer rate between the heating surface and the bulk of the liquid. At higher heat fluxes, more liquid is exposed to the surface with a higher temperature. Since the surface temperature is larger than the boiling temperature of the liquid, the rate of the evaporation is intensified, which not only increases the size of the bubble, but also intensifies the heat transfer rate from the surface to the bulk of the liquid. Please note that the larger bubbles create more agitation and microconvection heat transfer, which results in the intensification of the heat transfer coefficient.

4 Conclusion

An experimental investigation was conducted on the subcooled flow boiling heat transfer of a citric acid aqueous solution at 353 K and following conclusions have been made:

1. Two distinguishable heat transfer domains with different mechanisms were identified including the forced convective and nucleate boiling

heat transfer domains. In the forced convective heat transfer domain, the heat transfer coefficient was considerably smaller than that observed in the nucleate boiling domain. This was attributed to the formation of the bubbles in the nucleate boiling regime which enhanced the rate of heat transfer from the surface to the bulk of the liquid.

2. Heat and mass fluxes had a direct influence on the subcooled flow boiling heat transfer coefficient such that with an increase in the heat and mass fluxes, the flow boiling heat transfer coefficient increased.

3 It was found that with an increase in the volumetric concentration of citric acid in water, the heat transfer coefficient was decreased, which was attributed to the mixture effect and also the mass transfer resistance. This behavior was seen in both the forced convective and the nucleate boiling heat transfer regimes.

4. The Chen type model showed a 22% uncertainty against the nucleate boiling heat transfer coefficient obtained from the experiment, while the Dittus-Boelter correlation had a fair agreement with the experimental data within 12.83%. Also, a good agreement of 15% between the data obtained in the present research and those reported in the literature was obtained.

Received 11 September 2018

References

[1] Dhir V.: *Boiling heat transfer.* Annu. Rev. Fluid Mech. **30**(1998), 365–401.

[2] Stephan K., Abdelsalam M.: *Heat-transfer correlations for natural convection boiling.* Int. J. Heat Mass Tran. **23**(1980), 73–87.

[3] Liang G., Mudawar I.: textitReview of pool boiling enhancement with additives and nanofluids. Int.l J. Heat Mass Tran. **124**(2018), 423–453.

[4] Sarafraz M.: *Experimental investigation on pool boiling heat transfer to formic acid, propanol and 2-butanol pure liquids under the atmospheric pressure.* J. Appl. Fluid Mech. **6**(2013), 1, 73–79.

[5] Sarafraz M., Nikkhah V., Nakhjavani M., Arya A.: *Fouling formation and thermal performance of aqueous carbon nanotube nanofluid in a heat sink with rectangular parallel microchannel.* Appl. Therm. Eng. **123**(2017), 29–39.

[6] Sarafraz M., Peyghambarzadeh S., Alavifazel S.: *Enhancement of nucleate pool boiling heat transfer to dilute binary mixtures using endothermic chemical*

reactions around the smoothed horizontal cylinder. Heat Mass Transfer **48**(2012), 1755–1765.

[7] Das S.K., Putra N., Thiesen P., Roetzel W.: *Temperature dependence of thermal conductivity enhancement for nanofluids.* J. Heat Transf. **125**(2003), 567–5748.

[8] Sarafraz M., Peyghambarzadeh S., Alavi Fazel S., Vaeli N.: *Nucleate pool boiling heat transfer of binary nano mixtures under atmospheric pressure around a smooth horizontal cylinder.* Period. Polytech. Chem. Eng. **57**(2013), 1–2, 71–77.

[9] Sarafraz M.M., Hormozi F.: *Forced convective and nucleate flow boiling heat transfer to alumnia nanofluids.* Period. Polytech. Chem. Eng. **58**(2014), 37–4610.

[10] Alavi Fazel S., Sarafraz M., Arabi Shamsabadi A., Peyghambarzadeh S.: *Pool boiling heat transfer in diluted water.* Heat Transfer Eng. **34**(2013), 828–837.

[11] Fazel S.A., Shamsabadi A.A., Sarafraz M., Peyghambarzadeh S.: *Artificial boiling heat transfer in the free convection to carbonic acid solution.* Exp. Therm. Fluid Sci. **35**(2011), 645–652.

[12] Sarafraz M., Fazel A.S., Hasanzadeh Y., Arabshamsabadi A., Bahram S.: *Development of a new correlation for estimating pool boiling heat transfer coefficient of MEG/DEG/water ternary mixture.* CICEQ **18**(2012), 11–18.

[13] Liu Z., Winterton R.: *A general correlation for saturated and subcooled flow boiling in tubes and annuli, based on a nucleate pool boiling equation.* Int. J. Heat Mass Tran. **34**(1991), 2759–2766.

[14] Del Valle V.H.., Kenning D.: *Subcooled flow boiling at high heat flux.* Int. J. Heat Mass Tran. **28**(1985), 1907–1920.

[15] Benjamin R., Balakrishnan A.: *Nucleate pool boiling heat transfer of pure liquids at low to moderate heat fluxes.* Int. J. Heat Mass Tran. **39**(1996), 2495–2504.

[16] Bennett D.L., Chen J.C.: *Forced convective boiling in vertical tubes for saturated pure components and binary mixtures.* AIChE J. **26**(1980), 454–461.

[17] Sternling C., Tichacek L.: *Heat transfer coefficients for boiling mixtures: Experimental data for binary mixtures of large relative volatility.* Chem. Eng. Sci. **16**(1961), 297–337.

[18] Fazel S.A., Sarafraz M., Shamsabadi A.A., Peyghambarzadeh S.: *Pool boiling heat transfer in diluted water/glycerol binary solutions.* Heat Transfer Eng. **34**(2013), 828–837.

[19] Biglarian M., Gorji M.R., Pourmehran O., Domairry G.: *H2O based different nanofluids with unsteady condition and an external magnetic field on permeable channel heat transfer.* Int. J. Hydrogen Energ. **42**(2017), 22005–22014.

[20] Mohammadian M., Pourmehran O., Ju P.: *An iterative approach to obtaining the nonlinear frequency of a conservative oscillator with strong nonlinearities.* Int. Appl. Mech. **54**(2018), 470–479.

[21] Pourmehran O., Rahimi-Gorji M., Ganji D.D.: *Analysis of nanofluid flow in a porous media rotating system between two permeable sheets considering thermophoretic and Brownian motion.* Therm. Sci. **21**(2017), 6B, 3063–3073.

[22] Pourmehran O., Rahimi-Gorji M., Gorji-Bandpy M., Baou M.: *Comparison between the volumetric flow rate and pressure distribution for different kinds of sliding thrust bearing.* Propulsion Power Res. **4**(2015), 84–90.

[23] Pourmehran O., Sarafraz M., Rahimi-Gorji M., Ganji D.: *Rheological behaviour of various metal-based nano-fluids between rotating discs: a new insight.* J. Taiwan Inst. Chem. E. **88**(2018), 7, 37–48.

[24] Sarafraz M., Pourmehran O., Nikkhah V., Arya A.: *Pool boiling heat transfer to zinc oxide-ethylene glycol nano-suspension near the critical heat flux.* J. Mech. Sci. Technol. **32**(2018) 2309–2315.

[25] Tabassum R., Mehmood R., Pourmehran O., Akbar N., Gorji-Bandpy M.: *Impact of viscosity variation on oblique flow of Cu–H2O nanofluid.* In: Proc. Institution of Mechanical Engineers, Part E: J. Process Mech. Eng. **232**(2018), 622–631.

[26] Tavana M., Pourmehran O., Bandpy M.G., Sangarab J.A.: *Numerical analysis of fluid flow and heat transfer in microchannels with various internal fins.* IJAIM **3**(2015), 4, 227–230.

[27] Yousefi M., Pourmehran O., Gorji-Bandpy M., Inthavong K., Yeo L., Tu J.: *CFD simulation of aerosol delivery to a human lung via surface acoustic wave nebulization.* Biomech. Model. Mechan. **16**(2017), 2035–2050.

[28] Chen J.C.:Correlation for boiling heat transfer to saturated fluids in convective flow. Ind. Eng. Chem. Process Des. Dev. **5**(1966), 322–329.

[29] Nakhjavani M., Nikkhah V., Sarafraz M., Shoja S., Sarafraz M.: *Green synthesis of silver nanoparticles using green tea leaves: Experimental study on the morphological, rheological and antibacterial behaviour.* Heat Mass Transfer **53**(2017), 3201–3209.

[30] Sarafraz M., Hormozi F., Peyghambarzadeh S., Vaeli N.: *Upward flow boiling to DI-water and Cuo nanofluids inside the concentric annuli.* J. Appl. Fluid Mech. **8**(2015), 4, 651–659.

[31] Sarafraz M., Hormozi F., Silakhori M., Peyghambarzadeh S.: *On the fouling formation of functionalized and non-functionalized carbon nanotube nano-fluids under pool boiling condition.* Appl. Thermal Eng. **95**(2016), 433–444.

[32] Sarafraz M., Peyghambarzadeh S.: *Influence of thermodynamic models on the prediction of pool boiling heat transfer coefficient of dilute binary mixtures.* Int. Commun. Heat Mass **39**(2012), 1303–1310.

[33] Sarafraz M.M., Peyghambarzadeh S., Alavi F.S.: *Experimental studies on nucleate pool boiling heat transfer to ethanol/MEG/DEG ternary mixture as a new coolant.* CICEQ **18**(2012), 577–586.

[34] Racuciu M., Creanga D., Airinei A.: *Citric-acid-coated magnetite nanoparticles for biological applications.* Eur. Phys. J. E **21**(2006), 117–121.

[35] Nikkhah V., Sarafraz M., Hormozi F., Peyghambarzadeh S.: *Particulate fouling of CuO–water nanofluid at isothermal diffusive condition inside the conventional heat exchanger-experimental and modeling.* Exp. Therm. Fluid Sci. **60**(2015), 83–95.

[36] Peyghambarzadeh S., Sarafraz M., Vaeli N., Ameri E., Vatani A., Jamialahmadi M.: *Forced convective and subcooled flow boiling heat transfer to pure water and n-heptane in an annular heat exchanger.* Ann. Nucl. Energ. **53**(2013), 401–410.

[37] Sarafraz M., Arya A., Nikkhah V., Hormozi F.: *Thermal performance and viscosity of biologically produced silver/coconut oil nanofluids.* Chem. Biochem. Eng. **30**(2017), 489–500.

[38] Sarafraz M., Hormozi F.: *Scale formation and subcooled flow boiling heat transfer of CuO–water nanofluid inside the vertical annulus.* Exp. Therm. Fluid Sci. **52**(2014), 205–214.

[39] Sarafraz M., Hormozi F.: *Convective boiling and particulate fouling of stabilized CuO-ethylene glycol nanofluids inside the annular heat exchanger.* Int. Commun. Heat Mass **53**(2014), 116–123.

[40] Sarafraz M., Hormozi F.: *Comparatively experimental study on the boiling thermal performance of metal oxide and multi-walled carbon nanotube nanofluids.* Powder Technol. **287**(2016), 412–430.

[41] Sarafraz M., Hormozi F., Kamalgharibi M.: *Sedimentation and convective boiling heat transfer of CuO-water/ethylene glycol nanofluids.* Heat Mass Transfer **50**(2014), 1237–1249.

[42] Peyghambarzadeh S., Vatani A., Jamialahmadi M.: *Application of asymptotic model for the prediction of fouling rate of calcium sulfate under subcooled flow boiling.* Appl. Therm. Eng. **39**(2012), 105–113.

[43] Kline S., McClintock F.: *Describing Uncertainties in Single Sample Experiments.* Mech. Eng. **75**(1953), 1, 3–8.

[44] Sarafraz M., Arya A., Hormozi F., Nikkhah V.: *On the convective thermal performance of a CPU cooler working with liquid gallium and CuO/water nanofluid: A comparative study.* Appl. Therm. Eng. **112**(2017), 1373–1381.

[45] Sarafraz M., Arjomandi M.: *Demonstration of plausible application of gallium nano-suspension in microchannel solar thermal receiver: Experimental assessment of thermo-hydraulic performance of microchannel.* Int. Commun. Heat Mass **94**(2018), 39–46.

[46] Sarafraz M., Arjomandi M.: *Thermal performance analysis of a microchannel heat sink cooling with Copper Oxide-Indium (CuO/In) nano-suspensions at high-temperatures.* Appl. Therm. Eng. **137**(2018), 700–709.

[47] Sarafraz M., Arya H., Arjomandi M.: *Thermal and hydraulic analysis of a rectangular microchannel with gallium-copper oxide nano-suspension.* J. Mol. Liq. **263**(2018), 382–389.

[48] Gungor K.E., Winterton R.: *A general correlation for flow boiling in tubes and annuli.* Int. J. Heat Mass Tran. **29**(1986), 3, 351–358.

[49] Schroeder-Richter D., Bartsch G.: *Analytical calculation of DNB-superheating by a postulated thermo-mechanical effect of nucleate boiling.* Int. J. Multiphas. Flow **20**(1994), 1143–1167.

[50] Gnielinski V.: *New equations for heat and mass transfer in turbulent pipe and channel flow.* Int. Chem. Eng. **16**(1976), 359–368.

[51] Bier K., Gorenflo D., Salem M., Tanes Y.: *Pool boiling heat transfer and size of active nucleation centers for horizontal plates with different surface roughness.* In: Proc. 6th Int. Heat Transfer Conf., 1978, 151–156, DOI: 10.1615/IHTC6.3730.

[52] Gorenflo D., Sokol P., Caplanis S.: *Pool boiling heat transfer from single plain tubes to various hydrocarbons.* Int. J. Refrig. **13**(1990), 286–292.

[53] Sarafraz M., Peyghambarzadeh S.: *Experimental study on subcooled flow boiling heat transfer to water–diethylene glycol mixtures as a coolant inside a vertical annulus.* Exp. Therm. Fluid Sci. **50**(2013), 154–162.

[54] Sarafraz M.M.: *Nucleate pool boiling of aqueous solution of citric acid on a smoothed horizontal cylinder.* Heat Mass Transfer **48**(2012), 611–619.

[55] Peyghambarzadeh S., Jamialahmadi M., Alavi Fazel S., Azizi S.: *Experimental and theoretical study of pool boiling heat transfer to amine solutions.* Braz. J. Chem. Eng. **26**(2009), 33–43.

[56] Yu W., France D., Zhao W., Singh D., Smith R.: *Subcooled flow boiling heat transfer to water and ethylene glycol/water mixtures in a bottom-heated tube.* Exp. Heat Transfer **29**(2016), 593–614.

[57] Nikounezhad N., Nakhjavani M., Shirazi F.H.: *Generation of cisplatin-resistant ovarian cancer cell lines.* Iran. J. Pharma. Sci. **12**(2016), 11–20.

[58] Vakili N., Nakhjavani M., Mirzayi H., Shirazi F.: *Studying silibinin effect on human endothelial and hepatocarcinoma cell lines.* RPS **7**(2012), 174.

[59] Nikounezhad N., Nakhjavani M., Shirazi F.H.: *Cellular glutathione level does not predict ovarian cancer cells' resistance after initial or repeated exposure to cisplatin.* J. Exp. Therap. Oncol. 2017, 12.

[60] Shirazi F.H., Zarghi A., Kobarfard F., Zendehdel R., Nakhjavani M., Arfaiee S., Zebardast T., Mohebi S., Anjidani N., Ashtarinezhad A.: *Remarks in successful cellular investigations for fighting breast cancer using novel synthetic compounds.* In: Breast Cancer Focusing Tumor Microenvironment. Stem Cells and Metastasis (M. Gunduz, Ed.) Intech.Open, 2011, DOI: 10.5772/23005

[61] Nakhjavani M., Stewart D.J., Shirazi F.H.: *Effect of steroid and serum starvation on a human breast cancer adenocarcinoma cell line.* J. Exp. Therap. Oncol. 2017, 12.

[62] Arya H., Sarafraz M., Arjomandi M.: *Pool boiling under the magnetic environment: experimental study on the role of magnetism in particulate fouling and bubbling of iron oxide/ethylene glycol nano-suspension.* Heat Mass Transfer **55**(2019), 119–132.

[63] Arya H., Sarafraz M., Arjomandi M.: *Heat transfer and fluid flow of MgO/ethylene glycol in a corrugated heat exchanger.* J. Mech. Sci. Technol. **32**(2018), 3975–3982.

[64] Sarafraz M., Nikkhah V., Nakhjavani M., Arya A.: *Thermal performance of a heat sink microchannel working with biologically produced silver-water nanofluid: experimental assessment.* Exp. Therm. Fluid Sci. **91**(2018), 509–519.

[65] Sarafraz M., Shrestha E., Arya H., Arjomandi M.: *Experimental thermal energy assessment of a liquid metal eutectic in a microchannel heat exchanger equipped with a (10Hz/50Hz) resonator.* Appl. Therm. Eng. **148**(2019), 2, 578–590.